Graphene Growth Using a Solid Carbon Feedstock and Hydrogen

Hengxing Ji, Yufeng Hao, Yujie Ren, Matthew Charlton, Wi Hyoung Lee, Qingzhi Wu, Huifeng Li, Yanwu Zhu, Yaping Wu, Richard Piner, and Rodney S. Ruoff*

The Department of Mechanical Engineering and the Materials Science and Engineering Program, The University of Texas at Austin, 1 University Station C2200, Austin, Texas 78712-0292, United States

ABSTRACT Graphene has been grown on Cu at elevated temperatures with different carbon sources (gaseous hydrocarbons and solids such as polymers); however the detailed chemistry occurring at the Cu surface is not yet known. Here, we explored the possibility of obtaining graphene using amorphous-carbon thin films, without and with hydrogen gas added. Graphene is formed only in the presence of H_2(g), which strongly suggests that gaseous hydrocarbons and/or their intermediates are what yield graphene on Cu through the reaction of H_2(g) and the amorphous carbon. The large area, uniform monolayer graphene obtained had electron and hole mobilities of 2520 and 2050 $cm^2\ V^{-1}\ s^{-1}$, respectively.

KEYWORDS: graphene growth · amorphous carbon · hydrogen · hydrocarbon · mass spectroscopy

Graphene is of great interest owing to its atomically thin two-dimensional crystalline structure and unique electronic, optical, mechanical, and thermal properties.[1−8] As a basis for investigating its fundamental properties and realizing its applications, high-quality graphene with uniform coverage over a large area is needed. Graphene has been obtained by chemical vapor deposition (CVD) on transition metal surfaces and by segregation/precipitation from transition metals, mechanical exfoliation of graphite, thermal annealing of single-crystal SiC, and reduction of graphene oxide to yield "reduced graphene oxide" and not graphene *per se*.[1,4,9−18] CVD on Cu has recently provided uniform, relatively low defect graphene films transferrable to arbitrary substrates whose dimensions can meet the needs of, for example, the semiconductor industry.[14,19]

Recent attempts to grow graphene with different carbon sources, such as poly(methyl methacrylate), sucrose, benzene, methanol, and ethanol, suggest that Cu is a substrate that enables graphene growth from a variety of carbon-containing sources.[20−22] However, unlike Ni and Co, Cu is not able to induce graphitization of solid-state carbon according to the studies by *in situ* transmission electron microcopy (TEM) and differential scanning calorimetry (DSC).[23−25] The extremely low solubility of C in Cu[26] explains why graphene grows by surface-mediated mechanisms at a high temperature of exposure such as ~1000 °C,[14] rather than bulk processes such as precipitation upon cooling. The chemistry of different carbon precursors at the surface of Cu could be similar, namely, decomposition of a gas phase precursor, surface diffusion, nucleation, island growth, and island merger to yield a continuous graphene film. At this time we do not have a clear understanding of the detailed growth mechanisms for, for example, the growth of graphene from methane and hydrogen at elevated temperature on Cu.

Here, we explored the possibility of obtaining graphene from amorphous-carbon (a-C containing no H) thin films with thickness of tens of nanometers. We could not obtain graphene without simultaneous exposure to H_2(g), but with H_2(g) we could obtain high-quality monolayer graphene. Our work strongly suggests that the reaction of H_2(g) with the a-C film produced hydrocarbons and/or reactive hydrocarbon intermediates. It is such hydrocarbons and/or intermediates that yield graphene, through reaction of such species with the neat Cu substrate.

RESULTS AND DISCUSSION

A 20 nm thick amorphous carbon film was sputtered (graphite target, 99.999%, Kurt J. Lesker, item No. EJTCXXX503A4) onto a 25 μm thick Cu foil (99.8%, Alfa-Aesar, item No. 13382). The SEM image in Figure 1a of the carbon-coated Cu foil shows "ripples" on the Cu foil and regions with a relatively smooth surface. The Raman spectrum in Figure 1e shows the carbon film is amorphous before annealing. We attempted to obtain graphene by annealing this Cu foil having an a-C film at 1035 °C for 30 min in 2 sccm pure Ar. However, there were no

* Address correspondence to r.ruoff@mail.utexas.edu.

Received for review July 24, 2011 and accepted August 25, 2011.

Published online August 31, 2011
10.1021/nn202802x

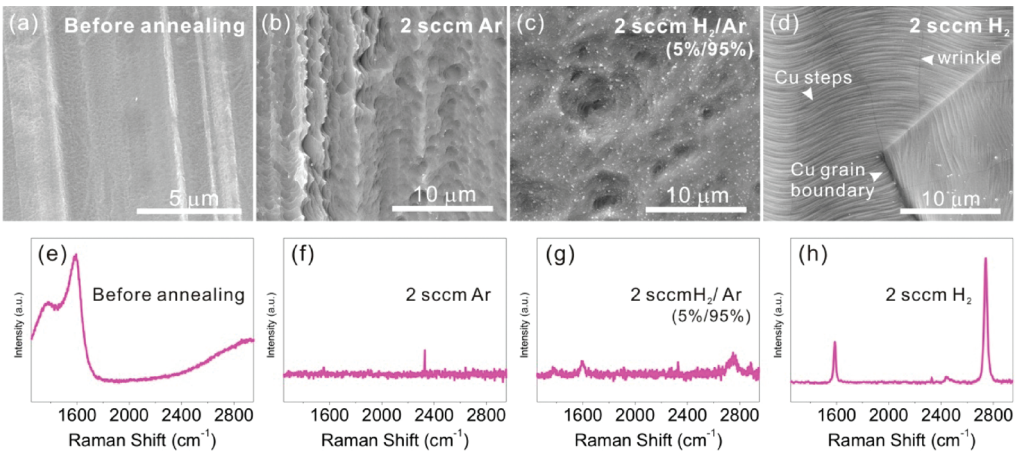

Figure 1. SEM images and Raman spectra (λ = 442 nm, 100× objective) of carbon-coated copper foil (a, e) before annealing and after annealing at 1035 °C for 30 min in (b, f) 2 sccm Ar, (c, g) 2 sccm H_2/Ar (5%/95% vol.) mixture, and (d, h) 2 sccm pure H_2, respectively. The Raman spectra were acquired at a same incident laser power and accumulation time.

indications of graphene on Cu (graphene wrinkles) in scanning electron microscopy images (SEM) acquired over the whole foil (Figure 1b). The Raman spectrum in Figure 1f shows only background noise, indicating that graphene was not produced and also that no a-C was left. This result is consistent with previous *in situ* TEM studies where it was stated that Cu does not bring about graphitization of solid-state carbon at temperatures of up to 950 °C.[23−25] When 2 sccm H_2/Ar mixture (5%/95% by volume) was used instead of pure Ar during the heat treatment, a very weak signal of sp^2-hybridized carbon in the Raman spectrum was obtained, as indicated by the small D, G, and 2D bands in Figure 1g. This result reveals that H_2(g) played a role in the "graphitization" of a-C at the Cu surface. Indeed, after heating the a-C-coated Cu foil at 1035 °C for 30 min in 2 sccm pure H_2(g), graphene was obtained on the Cu foil. In the SEM image, Figure 1d, graphene wrinkles as well as Cu grains and steps are clearly visible.[14] The graphene wrinkles are mostly perpendicular to steps on the Cu surface and some cross Cu grain boundaries, indicating a continuous graphene film. The Raman spectrum of the a-C-derived graphene in Figure 1h shows two large peaks, the G band at ~1580 cm^{-1} and the 2D band at ~2730 cm^{-1} (measured with 442 nm incident laser on Cu; Renishaw inVia). The I_{2D}/I_G ratio is about 3, and the full width at half-maximum (fwhm) of the 2D band is ~28 cm^{-1}, so the graphene is monolayer.[27,28] The D band that should appear at ~1365 cm^{-1} is nondetectable with our Raman system, indicating a low concentration of defects. Moreover, X-ray photoelectron spectroscopy (see Supporting Information, Figure S1) suggests a complete removal of the a-C thin film.

The only experimental difference in our three attempts is the type of gas flowing in the tube furnace when annealing the a-C-coated Cu foil. Graphene could not be obtained without simultaneous exposure

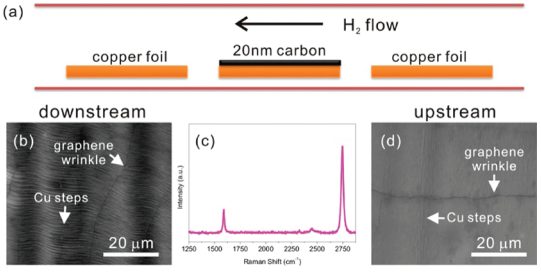

Figure 2. (a) Two Cu foils with no carbon coating were placed upstream and downstream of an a-C-coated Cu foil and heated at 1035 °C for 30 min in 2 sccm H_2(g). (b, d) SEM images and (c) a typical Raman spectrum of the neat Cu foils after the heat treatment.

to H_2(g), but with H_2(g) we could obtain monolayer graphene. This result suggests that H_2(g) plays a critical role. Previous studies reported that gaseous H_2 was able to react with graphite at temperatures below 1000 °C to generate hydrocarbons.[29,30] Therefore, we suspect that the carbon source that ultimately yields graphene is a gaseous hydrocarbon by reaction of H_2(g) with the a-C film.

As shown in Figure 2a, two Cu foil pieces without carbon coating were placed upstream and downstream of a 20 nm thick a-C-coated Cu foil (none of the 3 Cu foil pieces touched each other) and heated at 1035 °C for 30 min in 2 sccm H_2(g). The SEM images and the Raman spectrum shown in Figure 2b, c, and d prove the existence of monolayer graphene on both upstream and downstream Cu foils. Considering that the only carbon source was the a-C film on the middle Cu foil, three possible paths for carbon migration to feed the graphene growth on the downstream and upstream Cu foil pieces are (i) carbon atom surface diffusion on the Cu foil, (ii) carbon atoms/clusters being transported downstream and upstream as gaseous species, and/or (iii) hydrocarbons acting as the critical precursors. However, the gap between two adjacent

copper foils was several millimeters; thereby carbon diffusion through the Cu surface is not likely, as we never obtain graphene with isolated neat Cu foils under similar conditions. If C atoms/clusters were somehow evolving from the a-C film, they should rapidly react with H_2 at 1035 °C to form hydrocarbons or reactive intermediates such as methyl radicals and so on. We suggest that hydrocarbons (such as perhaps methane and ethane) and/or reactive hydrocarbon intermediates are the precursors for growth of graphene from the a-C film in the presence of H_2(g).

However, several fundamental questions, such as what are the main hydrocarbon products and when or at what temperatures are the hydrocarbons generated, are still yet to be answered. In order to answer these questions, we used a mass spectrometer (MS) to monitor the atmosphere in the tube furnace *in situ*. The MS (Stanford QMS 300) was equipped with a quadrupole mass analyzer, a separate pumping system, and a capillary sample probe. The capillary probe was placed 45 cm downstream of the flat temperature zone of the tube furnace. We focused on the partial pressure of the gas species monitored at the mass/charge (*m*/*e*) ratio of 15 (CH_3^+), since CH_4 could generate ions with a *m*/*e* of 15 (CH_3^+) and 16 (CH_4^+). O_2 and H_2O also generate ionized species with a *m*/*e* of 16 (O^+), but no other gases than CH_4 can generate ionized species of 15. In this way, the possible contribution of other gaseous molecules in the tube furnace, *e.g.*, H_2O, O_2, N_2, CO_2, CO, H_2, and Ar, can be eliminated. The partial pressures of the gases (CH_4, H_2, H_2O, O_2, Ar, *etc.*) were derived on the basis of the measurement of corresponding ionized species in the mass spectrometer, but not necessarily the practical partial pressure in the quartz tube used for graphene growth. We first measured the partial pressure of *m*/*e* equal to 15 while baking an empty quartz tube at 1035 °C in 2 sccm H_2(g) flow without a-C-coated Cu foils inside. The partial pressure as a function of time is shown in Figure 3a, which displays a straight line. A same straight line was also obtained if the valve between the capillary sample probe and the mass analyzer was turned off during measurement. After loading an a-C-coated Cu foil, we started the experiment according to the following procedures: (1) Started 2 sccm H_2 flow and then the mass spectrometer recording (time counting at 0); (2) kept the tube furnace at room temperature for 1200 s; (3) ramped the temperature to 1035 °C at a rate of around 60 °C min^{-1}; (4) kept the temperature of the tube furnace at 1035 °C for 1800 s; (5) started cooling at a rate of around 25 °C min^{-1}; (6) stopped H_2 flow and started Ar flow at 6600 s (when the temperature was around 400 °C). Figure 3b shows the partial pressure of CH_4 obtained by detecting ionized species at a *m*/*e* equal to 15 and the temperature of the tube furnace over the whole experimental procedure. A plateau appears at 2150 s when the temperature reaches around

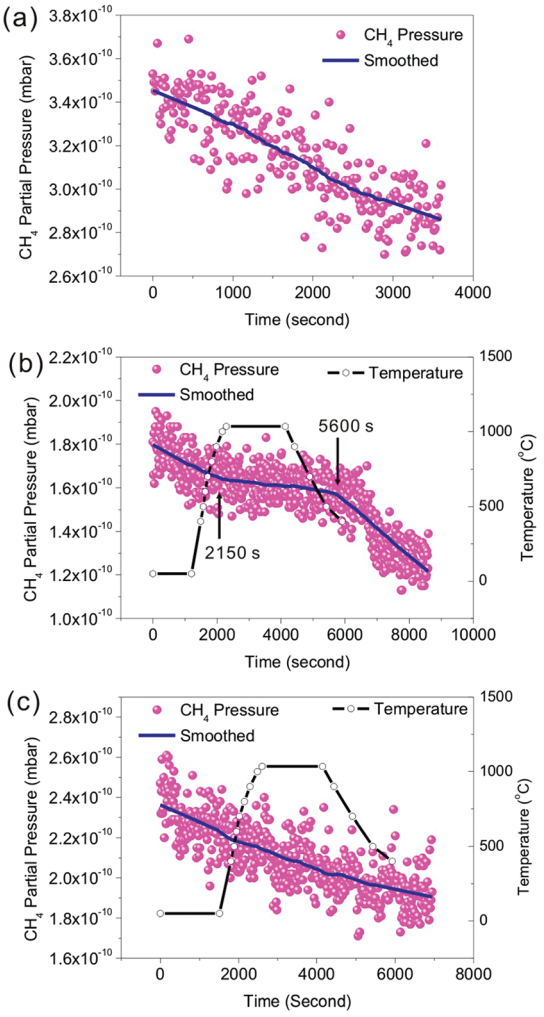

Figure 3. (a) CH_4 partial pressure in the tube furnace obtained while baking an empty quartz tube. (b) CH_4 partial pressure in the tube furnace while ramping the temperature from room temperature to 1035 °C, with an a-C-coated Cu foil in 2 sccm H_2(g). A plateau is presented from about 2150 s ($T \approx 1000$ °C) to 5600 s ($T < 500$ °C). (c) CH_4 partial pressure in the tube furnace while heating a neat Cu foil without a-C coating to 1035 °C in 2 sccm H_2(g). The black curves in panels (b) and (c) show the temperature profile of the furnace as a function of time.

1000 °C, and it ends at 5600 s when the temperature is below 500 °C. During heating of the a-C-coated Cu foil, the partial pressures of H_2 (*m*/*e* = 2), Ar (*m*/*e* = 40), O_2 (*m*/*e* = 32), and N_2 (*m*/*e* = 28) were also recorded (Figure S2). The partial pressures of O_2 and N_2 changed linearly over the whole experimental procedures, suggesting that the temperature and the changes in the type of gas flowing in the tube furnace did not contributed to the plateau in the curve of the partial pressure of CH_4 in Figure 3b. A control experiment was also carried out that involved heating a neat Cu foil without an a-C coating. The CH_4 partial pressure as a function of time (Figure 3c) is a straight line differing from the plateau shown in Figure 3b. Thus the plateau in Figure 3b is due to the reaction of the a-C coating with gaseous hydrogen. Considering that we do not

get graphene without exposure to H_2, our experimental results suggest that the carbon species that ultimately yield graphene on Cu are hydrocarbons, *e.g.*, CH_4, through the reaction of amorphous carbon and gaseous H_2 starting at around 1000 °C.

In this work, the original carbon source is the a-C thin film (typically 20 nm thick) that is restricted to the Cu foil surface, and the maximum amount of carbon sources is much less than that provided when graphene is grown with methane. Therefore, one concern could be whether the carbon sources are enough to generate graphene with high coverage and reasonable quality. We transferred the graphene that was grown from a-C thin films by using poly(methyl methacrylate) (PMMA)[14] to SiO_2/Si substrates to evaluate its quality. In the optical image in Figure 4a, optical contrast that originates from layer number difference is not observed, showing that the graphene film is uniform.[1] The Raman spectrum (λ = 532 nm, 100× objective, WITEC Alpha300) in Figure 4b shows a typical feature of monolayer graphene, with a 2D to G band intensity ratio of about 2.5 and a symmetric 2D band at ~2675 cm^{-1} with a fwhm of ~30 cm^{-1}.[27,28] The 2D map in Figure 4c shows a few brighter lines with a fwhm value of about 36 cm^{-1} corresponding to the wrinkles. The wrinkles might be due to the difference in the thermal expansion coefficient of Cu and graphene and/or to the transfer process.[14] The D band originates from an intervalley double resonance, which involves transitions near two inequivalent **K** points at neighboring corners of the first Brillouin zone of graphene and requires a defect for its activation.[27,31] The possible defects include graphene edges, grain boundaries, and sp^3-hybridized carbons that break the hexagonal structure of graphene. A higher defect concentration generates a more intense D band. Therefore, D band intensity is commonly used to monitor the quality of graphene. Figure 4d presents the D map generated from the region between 1200 and 1450 cm^{-1} (as marked in Figure 4b) where the D band should appear. For comparison, Figure 4e shows a Raman map generated from the region between 1800 and 2050 cm^{-1}, where only a background Raman signal was acquired. It is found that both Figure 4d and e have a similar intensity level and present a uniform signal intensity distribution. This suggests a nondetectable D band over the whole scanning region, which proves an excellent quality of the graphene film.

We studied the transport properties of a back-gated graphene field-effect transistor to further evaluate the quality of the graphene that was obtained from a-C thin film. The graphene was transferred onto a heavily doped Si substrate capped with 285 nm SiO_2. Au electrodes were deposited by thermal evaporation with a shadow mask. A transport channel of 1 mm in length and 5 mm in width was fabricated as shown in Figure 5a. Figure 5b presents the source–drain current

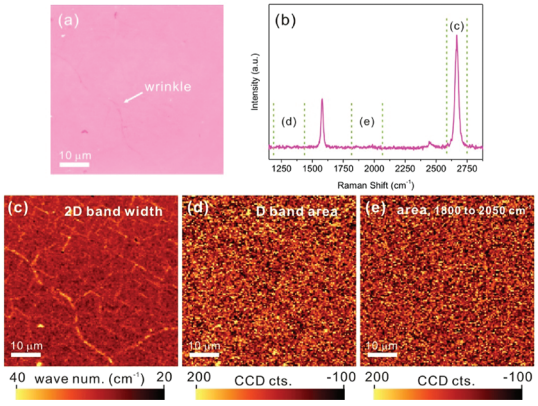

Figure 4. (a) Optical image of graphene film transferred onto a SiO_2/Si substrate. (b) Raman spectrum of this monolayer graphene, taken from the same region shown in (a). The regions marked with green dashed lines were used for creating Raman maps (λ = 532 nm, 100× objective) shown in (c)–(e). (c–e) Raman maps of the 2D band region (2600 to 2750 cm^{-1}), the D band region (1200 to 1450 cm^{-1}), and the region between 1800 and 2050 cm^{-1}, respectively.

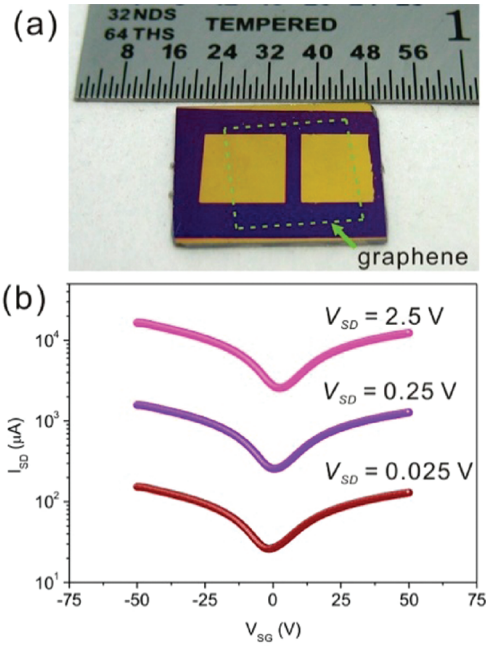

Figure 5. (a) Optical image of a graphene FET used for carrier mobility measurement. Graphene is marked with the green dashed square. The channel width and length between the two gold contacts was 1 and 5 mm, respectively. (b) Device source–drain current (I_{SD}) *versus* source–gate voltage (V_{SG}) measured with different source–drain voltage (V_{SD}) at 2 × 10^{-2} Torr. The hole and electron mobility at V_{SD} = 25 mV were calculated as 2520 and 2050 $cm^2 V^{-1} s^{-1}$, respectively.

(I_{SD}) with respect to the gate voltage (V_{SG}) measured at different source–drain bias (V_{SD}). The device shows a typical ambipolar transport behavior. The slight shift of the Dirac point between −1.0 and 2.5 V is a result of residual absorbents such as water and PMMA, which is commonly observed.[32] The I_{SD} increases linearly with increasing V_{SD} (Figure S3, in Supporting

Information), indicating the ohmic contact between the Au electrodes and graphene. The derived hole and electron mobilities at V_{SD} = 25 mV are ~2520 and ~2050 $cm^2 V^{-1} s^{-1}$, respectively.[33] A higher mobility of ~3700 $cm^2 V^{-1} s^{-1}$ is derived when a device with a shorter channel length of 50 μm was measured, as shown in Figure S4. This value (~3700 $cm^2 V^{-1} s^{-1}$) parallels those measured from the graphene with large single crystalline domains prepared by using methane as a carbon source[34,35] and is much higher than the reported values of graphene produced by other non-gaseous carbon sources.[20,36] In our earlier work,[35] we found that the very low pressure CVD process with methane as a carbon source could yield graphene with a domain size of up to 0.5 mm. The reasonably high quality of the graphene film that was proved by both Raman study and transport property may be attributed to the low pressure and uniform distribution of the hydrocarbon around the Cu foil, which is determined by the chemical reaction of the a-C thin film with H_2(g) occurring at the surface of Cu foil.

CONCLUSION

We investigated the growth of graphene with solid-state carbon feedstock. A mass spectrometer was applied in order to probe the atmosphere change in the tube furnace *in situ* during graphene growth. On the basis of our experimental results, we suggest that gaseous hydrocarbons, *e.g.*, CH_4, ultimately yield graphene on Cu through reaction of H_2(g) with the a-C film. The basic understanding presented in this paper can be helpful to interpret the graphene growth with a variety of carbon-containing sources on Cu.

METHODS

Amorphous carbon was deposited on a 25 μm thick Cu foil (99.8%, Alfa-Aesar) at a deposition rate of around 0.3 Å/s by RF-sputter with a graphite target (99.999%, Kurt J. Lesker) at 200 W and 2.5 × 10^{-3} Torr Ar. The thickness of the carbon thin film was monitored by a quartz film-thickness detector. Then the a-C-coated Cu foil was cut into, typically, 1 cm × 5 cm stripes and loaded into a hot wall tube furnace consisting of a 22 mm diameter fused quartz tube heated in a split furnace. A typical growth process was

(1) loading the a-C-coated Cu foil in to the tube furnace, evacuating, backfilling with H_2, and maintaining a pressure of 20 mtorr with a H_2 flow of 2 sccm;

(2) heating the tube furnace to 1035 °C in 13 min and maintaining the temperature of 1035 °C for 30 min;

(3) cooling to room temperature at a rate varied between 20 °C/min and >100 °C/min, which resulted in films with no discernible difference.

Graphene films were transferred onto 285 nm SiO_2/Si substrates using poly(methyl methacrylate)[1] for optical microscopy and micro-Raman imaging spectroscopy.

The SEM images were obtained with Quanta F600 ESEM at 30 kV. The Raman spectra of graphene on Cu were measured by Renishaw inVia with a 442 nm laser and 100× objective lens, and the Raman spectra of graphene on SiO_2/Si were measured by WITEC Alpha300 with a 532 nm laser and 100× objective lens. XPS was conducted with a Kratos AXIS Ultra DLD equipped with a monochromatic Al Kα source. FET measurements were performed by a programmable voltage source, Keithley 2611A, and digital voltmeter/ammeter, Keithley 6221 and 6514.

Acknowledgment. We appreciate support from the National Science Foundation (Grant No. 1006350), the Nanoelectronic Research Initiative−SouthWest Academy of Nanoelectronics (NRI-SWAN), and the Office of Naval Research.

Supporting Information Available: Figures S1−4. This material is available free of charge *via* the Internet at http://pubs.acs.org.

REFERENCES AND NOTES

1. Novoselov, K. S.; Geim, A. K.; Morozov, S. V.; Jiang, D.; Zhang, Y.; Dubonos, S. V.; Grigorieva, I. V.; Firsov, A. A. Electric Field Effect in Atomically Thin Carbon Films. *Science* **2004**, *306*, 666–669.
2. Novoselov, K. S.; Geim, A. K.; Morozov, S. V.; Jiang, D.; Katsnelson, M. I.; Grigorieva, I. V.; Dubonos, S. V.; Firsov, A. A. Two-Dimensional Gas of Massless Dirac Fermions in Graphene. *Nature* **2005**, *438*, 197–200.
3. Geim, A. K.; Novoselov, K. S. The Rise of Graphene. *Nat. Mater.* **2007**, *6*, 183–191.
4. Zhu, Y. W.; Murali, S.; Cai, W. W.; Li, X. S.; Suk, J. W.; Potts, J. R.; Ruoff, R. S. Graphene and Graphene Oxide: Synthesis, Properties, and Applications. *Adv. Mater.* **2010**, *22*, 3906–3924.
5. Dreyer, D. R.; Ruoff, R. S.; Bielawski, C. W. From Conception to Realization: An Historial Account of Graphene and Some Perspectives for Its Future. *Angew. Chem., Int. Ed.* **2010**, *49*, 9336–9344.
6. Geim, A. K. Graphene: Status and Prospects. *Science* **2009**, *324*, 1530–1534.
7. Zhang, Y. B.; Tan, Y. W.; Stormer, H. L.; Kim, P. Experimental Observation of the Quantum Hall Effect and Berry's Phase in Graphene. *Nature* **2005**, *438*, 201–204.
8. Schwierz, F. Graphene Transistors. *Nat. Nanotechnol.* **2010**, *5*, 487–496.
9. Berger, C.; Song, Z. M.; Li, X. B.; Wu, X. S.; Brown, N.; Naud, C.; Mayou, D.; Li, T. B.; Hass, J.; Marchenkov, A. N.; *et al.* Electronic Confinement and Coherence in Patterned Epitaxial Graphene. *Science* **2006**, *312*, 1191–1196.
10. Mallet, P.; Varchon, F.; Naud, C.; Magaud, L.; Berger, C.; Veuillen, J. Y. Electron States of Mono- and Bilayer Graphene on SiC Probed by Scanning-Tunneling Microscopy. *Phys. Rev. B* **2007**, *76*, 041403.
11. Varchon, F.; Feng, R.; Hass, J.; Li, X.; Nguyen, B. N.; Naud, C.; Mallet, P.; Veuillen, J. Y.; Berger, C.; Conrad, E. H.; *et al.* Electronic Structure of Epitaxial Graphene Layers on SiC: Effect of the Substrate. *Phys. Rev. Lett.* **2007**, *99*, 126805.
12. Hernandez, Y.; Nicolosi, V.; Lotya, M.; Blighe, F. M.; Sun, Z. Y.; De, S.; McGovern, I. T.; Holland, B.; Byrne, M.; Gun'ko, Y. K.; *et al.* High-Yield Production of Graphene by Liquid-Phase Exfoliation of Graphite. *Nat. Nanotechnol.* **2008**, *3*, 563–568.
13. Kim, K. S.; Zhao, Y.; Jang, H.; Lee, S. Y.; Kim, J. M.; Kim, K. S.; Ahn, J. H.; Kim, P.; Choi, J. Y.; Hong, B. H. Large-Scale Pattern Growth of Graphene Films for Stretchable Transparent Electrodes. *Nature* **2009**, *457*, 706–710.
14. Li, X. S.; Cai, W. W.; An, J. H.; Kim, S.; Nah, J.; Yang, D. X.; Piner, R.; Velamakanni, A.; Jung, I.; Tutuc, E.; *et al.* Large-Area Synthesis of High-Quality and Uniform Graphene Films on Copper Foils. *Science* **2009**, *324*, 1312–1314.
15. Park, S.; Ruoff, R. S. Chemical Methods for the Production of Graphenes. *Nat. Nanotechnol.* **2009**, *4*, 217–224.
16. Stankovich, S.; Dikin, D. A.; Piner, R. D.; Kohlhaas, K. A.; Kleinhammes, A.; Jia, Y.; Wu, Y.; Nguyen, S. T.; Ruoff, R. S. Synthesis of Graphene-Based Nanosheets via Chemical Reduction of Exfoliated Graphite Oxide. *Carbon* **2007**, *45*, 1558–1565.

17. Liu, N.; Fu, L.; Dai, B. Y.; Yan, K.; Liu, X.; Zhao, R. Q.; Zhang, Y. F.; Liu, Z. F. Universal Segregation Growth Approach to Wafer-Size Graphene from Non-Noble Metals. *Nano Lett.* **2010**, *11*, 297–303.
18. Pollard, A. J.; Nair, R. R.; Sabki, S. N.; Staddon, C. R.; Perdigao, L. M. A.; Hsu, C. H.; Garfitt, J. M.; Gangopadhyay, S.; Gleeson, H. F.; Geim, A. K.; *et al*. Formation of Monolayer Graphene by Annealing Sacrificial Nickel Thin Films. *J. Phys. Chem. C* **2009**, *113*, 16565–16567.
19. Bae, S.; Kim, H.; Lee, Y.; Xu, X. F.; Park, J. S.; Zheng, Y.; Balakrishnan, J.; Lei, T.; Kim, H. R.; Song, Y. I.; *et al*. Roll-to-Roll Production of 30-in. Graphene Films for Transparent Electrodes. *Nat. Nanotechnol.* **2010**, *5*, 574–578.
20. Sun, Z. Z.; Yan, Z.; Yao, J.; Beitler, E.; Zhu, Y.; Tour, J. M. Growth of Graphene from Solid Carbon Sources. *Nature* **2010**, *468*, 549–552.
21. Li, Z. C.; Wu, P.; Wang, C. X.; Fan, X. D.; Zhang, W. H.; Zhai, X. F.; Zeng, C. G.; Li, Z. Y.; Yang, J. L.; Hou, J. G. Low-Temperature Growth of Graphene by Chemical Vapor Deposition Using Solid and Liquid Carbon Sources. *ACS Nano* **2011**, *5*, 3385–3390.
22. Guermoune, A.; Chari, T.; Popescu, F.; Sabri, S. S.; Guillemette, J.; Skulason, H. S.; Szkopek, T.; Siaj, M. Chemical Vapor Deposition Synthesis of Graphene on Copper with Methanol, Ethanol, and Propanol Precursors. *Carbon* **2011**, *49*, 4204–4210.
23. Sinclair, R.; Itoh, T.; Chin, R. In situ TEM Studies of Metal-Carbon Reactions. *Microsc. Microanal.* **2002**, *8*, 288–304.
24. Zheng, M.; Takei, K.; Hsia, B.; Fang, H.; Zhang, X. B.; Ferralis, N.; Ko, H.; Chueh, Y. L.; Zhang, Y. G.; Maboudian, R.; *et al*. Metal-Catalyzed Crystallization of Amorphous Carbon to Graphene. *Appl. Phys. Lett.* **2010**, *96*, 063110.
25. Rodriguez-Manzo, J. A.; Pham-Huu, C.; Banhart, F. Graphene Growth by a Metal-Catalyzed Solid-State Transformation of Amorphous Carbon. *ACS Nano* **2011**, *5*, 1529–1534.
26. Lopez, G. A.; Mittemeijer, E. The Solubility of C in Solid Cu. *Scr. Mater.* **2004**, *51*, 1–5.
27. Ferrari, A. C. Raman Spectroscopy of Graphene and Graphite: Disorder, Electron-Phonon Coupling, Doping and Monadiabatic Effects. *Solid State Commun.* **2007**, *143*, 47–57.
28. Malard, L. M.; Pimenta, M. A.; Dresselhaus, G.; Dresselhaus, M. S. Raman Spectroscopy in Graphene. *Phys. Rep.* **2009**, *473*, 51–87.
29. Szab, Z. The Examination of a System Carbon and Hydrogen in the Temperature Range 1100−2600 °C. *J. Am. Chem. Soc.* **1950**, *72*, 3497–3502.
30. Breisacher, P.; Marx, P. C. The Hydrogen-Graphite Reaction between 360 and 800 °C. *J. Am. Chem. Soc.* **1963**, *85*, 3518–3519.
31. Ding, F.; Ji, H. X.; Chen, Y. H.; Herklotz, A.; Dorr, K.; Mei, Y. F.; Rastelli, A.; Schmidt, O. G. Stretchable Graphene: A Close Look at Fundamental Parameters through Biaxial Straining. *Nano Lett.* **2011**, *10*, 3453–3458.
32. Schedin, F.; Geim, A. K.; Morozov, S. V.; Hill, E. W.; Blake, P.; Katsnelson, M. I.; Novoselov, K. S. Detection of Individual Gas Molecules Adsorbed on Graphene. *Nat. Mater.* **2007**, *6*, 652–655.
33. Liang, X.; Fu, Z.; Chou, S. Y. Graphene Transistors Fabricated via Transfer-Printing in Device Active-Areas on Large Wafer. *Nano Lett.* **2007**, *7*, 3840–3844.
34. Li, X. S.; Magnuson, C. W.; Venugopal, A.; An, J. H.; Suk, J. W.; Han, B. Y.; Borysiak, M.; Cai, W. W.; Velamakanni, A.; Zhu, Y. W.; *et al*. Graphene Films with Large Domain Size by a Two-Step Chemical Vapor Deposition Process. *Nano Lett.* **2010**, *10*, 4328–4334.
35. Li, X. S.; Magnuson, C. W.; Venugopal, A.; Tromp, R. M.; Hannon, J. B.; Vogel, E. M.; Colombo, L.; Ruoff, R. S. Large-Area Graphene Single Crystals Grown by Low-Pressure Chemical Vapor Deposition of Methane on Copper. *J. Am. Chem. Soc.* **2010**, *133*, 2816–2819.
36. Jin, Z.; Yao, J.; Kittrell, C.; Tour, J. M. Large-Scale Growth and Characterizations of Nitrogen-Doped Monolayer Graphene Sheets. *ACS Nano* **2011**, *5*, 4112–4117.